# PREDICTING PERMEABILITY THROUGH 3D PORE-SPACE IMAGES RECONSTRUCTED USING MULTIPLE-POINT STATISTICS

H. Okabe [1,2] and M.J. Blunt[1]

[1] Department of Earth Science and Engineering, Imperial College London, SW7 2AZ, UK

[2] Japan Oil, Gas and Metals National Corporation, 1-2-2 Hamada, Mihama-ku, Chiba-shi, Chiba, 261-0025, Japan

*This paper was prepared for presentation at the International Symposium of the Society of Core Analysts held in Abu Dhabi, UAE, 5-9 October 2004*

## ABSTRACT

Pore-scale network modeling can predict multiphase flow properties with arbitrary wetting conditions if the network represents the geology of the sample accurately. Such pore-scale modeling uses topologically disordered networks that realistically represent the pore structure. To generate the network it is first necessary to have a three-dimensional voxel-based pore-space representation that is constructed by either a direct imaging technique such as micro-CT scanning, stochastic methods, or object-based approaches. Micro-CT scanning is the most promising among these three approaches since it is the most direct. However, its resolution – a few microns – means that for many rocks, particularly carbonates, significant porosity cannot be imaged. Furthermore, alternative approaches, such as reconstruction through simulating the geological processes by which the rock was formed, such as sedimentation and diagenesis, may be problematic for many materials whose depositional and diagenetic history is uncertain or complex. Statistical reconstruction is more general and is not limited by the pore size. Statistics of the pore space are obtained from readily available experimental data such as thin-section images. Using only single and two-point statistics in the reconstruction often underestimates the pore connectivity, especially for low porosity materials.

We use multiple-point statistics for pore space reconstruction that preserves higher-order information, describing the statistical relation between multiple spatial locations. This is a general method that gives images that preserve typical patterns of the void space seen in thin sections. The method is tested on a carbonate sample from the Middle East. Permeability is predicted directly on the 3D images using the lattice Boltzmann method. The numerically estimated results are in good agreement with experimentally measured permeability. Furthermore, this method provides an important input for the creation of geologically realistic networks for pore-scale modeling to predict multiphase flow properties.

## INTRODUCTION

Transport properties such as relative permeability and capillary pressure functions define flow behavior in porous media. These functions critically depend on the geometry and topology of the pore space, the physical relationship between rock grains and the fluids, and the conditions imposed by the flow process. A quantitative prediction of petrophysical properties in porous media, such as reservoir rocks, frequently employs representative microscopic models of the microstructure as input. It is necessary that proper pore structural information is supplied as input to predict fluid flow properties using network models [1] or other approaches, such as the lattice-Boltzmann method [2].

The reconstruction of 3D porous media is of great interest in a wide variety of fields, including earth science and engineering, biology, and medicine. Several methods have been proposed to generate 3D pore space images. A series of 2D sections can be combined to form a 3D image. This is a laborious operation limited by the impossibility of preparing cross sections with a spacing of less than about 10μm [3]. However, recent advances, such as the use of a focused ion beam [4, 5] allow higher resolution images (sub-micron size) to be constructed. Another approach is to use non-destructive X-ray computed microtomography [6] to image a 3D pore space directly at resolutions of around a micron. However, this resolution is not sufficient to image the sub-micron size pores that are abundant in carbonates, which can be imaged by 2D techniques such as scanning electron microscopy (SEM). The sub-micron structures of real rocks have been studied using laser scanning confocal microscopy [7]. It has, however, limited ability to penetrate solid materials. In the absence of higher resolution 3D images, reconstructions from readily available 2D microscopic images are the only viable alternative.

**Numerical reconstructions**

2D high-resolution images provide important geometrical properties such as the porosity and typical patterns. Based on the information extracted from 2D images, one promising way is to reconstruct the porous medium by modeling the geological process by which it was made [8-10]. Although the process-based reconstruction is general and possible to reproduce the long-range connectivity, there are many systems for which the process-based reconstruction is very difficult to apply. For instance, for many carbonates it would be very complex to use a process-based method that mimics the geological history involving the sedimentation of irregular shapes followed by significant compaction, dissolution and reaction [11]. In these cases it is necessary to find another approach to generate a pore space representation. One method is to use statistical techniques to produce a 3D image from 2D thin section image analysis, as mentioned before. Traditionally two-point statistics have been used to achieve this. However, these images often fail to reproduce the long-range connectivity of the pore space, especially for low porosity materials. We have shown the ability to reconstruct a geologically realistic pore-space structure by the multiple-point statistical technique [12], which uses higher order information [13, 14]. One key aspect of the work is the proper selection of the multiple-point statistics to reproduce satisfactory images. In the previous paper [12], we studied sandstone and showed that the long-range connectivity of the pore space was appropriately reproduced. In this paper, we apply the method to a carbonate rock since the method is suitable for any material, including those with sub-micron structures. The reconstructed 3D pore structures are tested by predicting permeability using the lattice-Boltzmann method. In addition permeabilities of the structures are predicted directly from 2D images using an extension of the effective medium approximation [15].

## MULTIPLE-POINT STATISTICS METHOD

Multiple-point statistics cannot be inferred from sparse data; their inference requires a densely and regularly sampled training image describing the geometries expected to exist in the real structure. For example, photographs of outcrops at the field scale and microscope images at the pore scale can be used as training images. The procedure mainly consists of two steps: (1) extracting multiple-point statistics from training images and (2) pattern reproduction [13, 14].

The training image in Figure 1 is scanned using a template *t* composed of $n_t$ locations $\vec{u}_\alpha$ and a central location $\vec{u}$:

$$\vec{u}_\alpha = \vec{u} + \vec{h}_\alpha \quad \alpha = 1,...,n_t \tag{1}$$

where the $\vec{h}_\alpha$ are the vectors describing the template. For instance, in Figure 1(b), $\vec{h}_\alpha$ are the 80 vectors of the square 9 × 9 template. The template is used to scan the training image and collect the pattern at each location $\vec{u}$. The pattern is defined by

$$pattern(u) = \left\{ i(\vec{u}); i(\vec{u} + \vec{h}_\alpha),\ \alpha = 1,...,n_t \right\} \tag{2}$$

where $i(\vec{u})$ is the data value at the point within the template. Each point in the template has a number to identify the pattern and to store the pattern in memory. The set of all patterns scanned from the training image results in a *training data set*

$$Set = \left\{ pattern(u_j),\ \ j = 1,..., N_t \right\} \tag{3}$$

where *Set* refers to the training data set constructed with the template *t*. $N_t$ is the number of different central locations of template *t* over the training image.

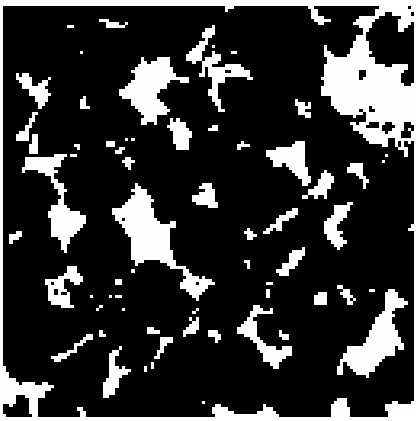

(a) Training image

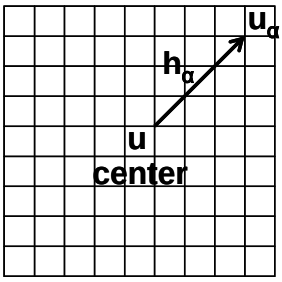


(b) Template

Figure 1. (a) An example of a training image (a thin section of Berea sandstone with a porosity of 0.177, $128^2$ pixels). The pore space is shown white and the grain black. The resolution of the image is 10μm/pixel. (b) A 9 × 9 template to capture multiple-point statistics. The training image is scanned and each occurrence of any possible patterns of void space and solid is recorded.

The selection of the template is important and various template sizes $n_t$ should be tried in order to reproduce the structure. This can be examined by a visual inspection of reconstructed images and predicting the autocorrelation function. We use binary thin section images that have only void or solid. A detailed discussion of the training image can be found in the Rock Sample section.

Multiple-point statistics are actually probabilities of occurrence of patterns. The probability of occurrence of any pattern $pattern_n$ associated with the data template *t* can be inferred from the training image by counting the number $c(pattern_n)$ of replicates of $pattern_n$ found in the training image. A replicate should have the same geometry and the same data values as $pattern_n$. The multiple-point statistics can be identified to the proportion:

$$\Pr(pattern_n) \approx c(pattern_n)/N_n \tag{4}$$

where $N_n$ is the size of the pattern. The key to this algorithm is the determination of the local conditional probability distribution functions (cpdf). We need to evaluate the probability that the unknown attribute value $i(\vec{u})$ takes any of 2 possible states – void or solid – given *n* nearest data during the reproduction at any unsampled location $\vec{u}$. If multiple-point statistics are available, then the conditioning of $i(\vec{u})$ to the single global pattern $pattern_n$ can be considered, and the conditional probability can be identified to the training proportion. The cpdf is inferred directly and consistently from the training image. The multiple-point statistics, the geometrical structures in other words, are borrowed directly from the training image.

This approach can theoretically apply to a 3D field when 3D structural information is available. Since it is difficult or impossible to measure 3D sub-micron scale data, as mentioned above, our only alternative is to use 2D images to measure multiple-point statistics. In our case, in order to generate a 3D structure from 2D information, measured multiple-point statistics on one plane are rotated 90 degrees around each principal axis. In other words, measured statistics on the XY plane are transformed to the YZ and the XZ planes with an assumption of isotropy in orthogonal directions.

In the presence of large-scale structures, the use of a single limited-size template would not suffice to model the large-scale characteristics observed in the training image. The template size can be theoretically expanded to match the largest structure in the training

image. However, the template size is constrained by memory limitations in the numerical simulation. An alternative approach can be introduced by a sort of multigrid simulation. Four different sized templates are used to scan the training image, resulting in four different data sets *Set* $t_1$, *Set* $t_2$, *Set* $t_3$ and *Set* $t_4$. Larger scale templates can simply be expanded from the small-scale template. In a multigrid system, a simulation is first performed on the coarsest grid. Once the coarse simulation is finished, the simulated values are assigned to the correct grid locations on the finer grid, and are used as conditioning data on the finer grid. When large-scale structures exist in the training image, this multigrid approach captures the large-scale multiple-point statistics effectively while requiring relatively little memory.

To summarize multiple-point statistics reconstruction: a training image provides the characteristic pattern and cpdf within a designated template, then each point is reproduced using local surrounding points already reproduced and statistical information derived from a training image and a template.

## NUMERICAL METHODS

### The effective medium approximation (EMA)

If the 3D microstructure is available, solving the Navier-Stokes equations by, for instance, the lattice-Boltzmann method can yield the permeability with reasonable accuracy at the expense of extensive data collection and computation. On the other hand, a quick estimation of permeability directly from a 2D image can be made by the effective medium approximation (EMA) [16]. First the pore size distribution is estimated from the 2D image. The perimeter, $P$ and area, $A$ of each pore in a 2D image are estimated by the image analysis in order to approximate the hydraulic radius, $C_i=A^3/P^2$. We use the extended version of the EMA with the use of a hydraulic constriction and a stereological correction factor for area and perimeter, which are multiplied to the hydraulic radius in order to obtain a more realistic conductance [15, 17]. The stereological correction factor takes into account idealized cylindrical pores in 2D and 3D. EMA replaces each conductance $C_i$ in a pore network with the effective value $C_{eff}$. The effective conductance can be found by solving the following equation.

$$\sum_{i=1}^{N} \frac{C_{eff} - C_i}{(z/2-1)C_{eff} + C_i} = 0 \tag{5}$$

where $z$ is the coordination number that represents the number of throats connected to

each pore. Assuming a cubic network ($z$ = 6), the permeability is calculated using

$$k = \frac{NC_{eff}}{1.47A_{total}} \tag{6}$$

where $N$ is the number of conductors in the designated direction and $A_{total}$ is total area. 1.47 is the number density correction factor, which is derived for the number density of pore intersections made by an arbitrary slice in a cubic network. More details can be found in [15, 17].

**The lattice-Boltzmann method (LBM)**

The lattice-Boltzmann method (LBM) provides a good approximation to solutions of the Navier-Stokes equations using a parallel and efficient algorithm that readily accommodates complex boundaries, as encountered in porous media [18]. We have developed a 3D two-phase LB model based on the 2D two-phase LB model proposed by Grunau *et al.* [19]. The model has been validated by precise comparisons with empirical equations, analytical solutions, and experiments [20]. We use this LBM as a single-phase flow simulator in this study. The model for the single phase can be described as

$$f_i\left(x+e_i,t+1\right)-f_i\left(x,t\right)=-\frac{1}{\tau}\left[f_i\left(x,t\right)-f_i^{(eq)}\left(x,t\right)\right] \tag{7}$$

where $f_i(\mathbf{x},t)$ is the particle distribution function at space **x** and time $t$ along the $i$-th direction ($i$=0,1,2, …, 18 in our case) and $\mathbf{e}_i$ is the local particle velocity. The right term is the BGK collision operator [21], which is widely used due to its simplicity and represents the relaxation process to local equilibrium $f_i^{(eq)}$. $\tau$ is the single time relaxation parameter. We use a three-dimensional nineteen velocity model, D3Q19, which includes a rest vector.

The bounce-back scheme at walls is used to obtain no-slip velocity conditions. By the bounce-back scheme, when a particle distribution moves to a wall, the particle distribution scatters back to the node it came from. This simple boundary scheme allows the LBM to simulate fluid flows in complicated geometries. The flow field is computed using periodic boundary conditions.

## ROCK SAMPLE

The carbonate rock sample used in our study consists of limestone and is classified as bioclastic packstone/grainstone. The core plug of this rock with 38 mm in diameter and

70 mm long has a porosity of 0.318 and a permeability of 6.7 md [22]. As described before, there is no 3D microstructure for this rock since the mean pore size is smaller than the resolution of micro-CT scanning. Part of 2D thin section image (512×512) shown in Figure 2 is used as training image in order to reconstruct 3D structures by our method.

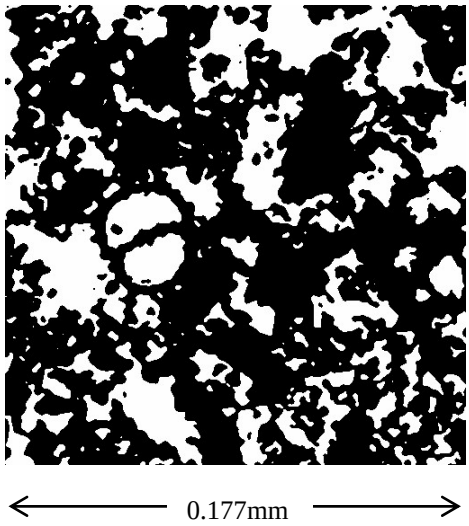


Figure 2. Binarized 2D thin section image of the carbonate rock (512×512 pixels, 0.345μm/pixel) with a porosity of 0.331. The void space is white and the solid black.

## RESULTS

### Permeability estimation by EMA

The permeability of the sample is estimated directly from the 2D image. The hydraulic constriction factor of *0.44* and the stereological correction factor of *3/8* is multiplied to the measured hydraulic radius [15]. Assuming a cubic network, the coordination number of six is used in our estimations. We know the assumption of cubic pore network might be over-simplified; however, EMA is useful to estimate permeability without massive computational requirements and to evaluate a 2D image in advance of 3D reconstruction. Estimations of permeabilities for the carbonate rock are in reasonably good agreement with experiment data as shown in Table 1, although the size of the samples is different.

Table 1. Computed permeabilities using the EMA and the LBM for the carbonates. In addition, results for Berea sandstone shown in Figure 1(a) are listed for comparison.

| | Experiment | | Computed permeability, md | | 3D reconstructed |
|---|---|---|---|---|---|
| Sample No. | Porosity | Permeability, md | By EMA | By LBM | Porosity |
| Carbonate | 0.318 | 6.7 | 6.05 | 19.8 | 0.318 |
| Berea | 0.178 | 1100 | 1448 | 1274 | 0.178 |

**Template selection**

We use four different sized templates with the same 9×9 square shape, spanning 9×9, 18×18, 27×27 and 36×36 pixels. A larger template can capture large structures; however, it takes much more CPU time and introduces more noise if the training image does not provide sufficient statistics. We decided to use a 9×9 template mainly in terms of CPU time after considering larger and smaller templates – this gave the optimum combination: less CPU time compared with a larger 11×11 template which doubles CPU time, less noise and preserving larger features than the use of a smaller 7×7 template. Advancements of CPU and a computer memory will allow us to use a larger template to capture large patterns.

**Unconditional 3D reconstruction by the multiple-point statistics method**

Figure 3 shows 2D cuts and 3D reconstructed image of the rock without conditioning data. There is unrealistic noise in the images due to insufficient statistics provided by 2D images. For example, if similar patterns in the training image cannot be found, the porosity value is simply used as a probability to reconstruct the voxel. This will lead to a noisy image. However, characteristic structures of the void space are reasonably preserved. General image processing of dilation and erosion operations is applied to reconstructed images to remove noise and smooth the boundary for the LBM simulation and a future network generation. Porosity is preserved in this operation.

**Permeability by LBM**

Since no microtomographic image of the carbonate rock is available, the LBM simulation is a convenient way to assess the reconstructed structures. The computed permeabilities of the reconstructed microstructures averaged over five realizations are listed in Table 1. Although the value for the carbonates is overestimated from the experimental

permeability, the estimation is good considering the significant size difference between reconstructed images and the experimental sample. Larger training images can capture more statistics and may produce more realistic images with similar permeability values to the experiment. In addition more information, such as several thin section images and multi-orientation thin section images may improve the results.

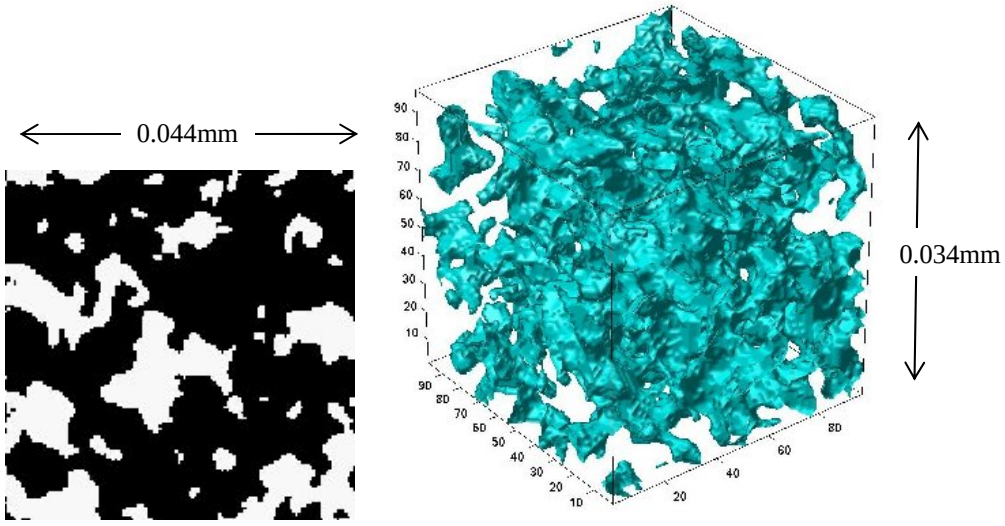


Figure 3. A 2D cut ($\phi$=0.296) through an unconditional reconstruction of carbonate rock and its subgrid of 3D image with $\phi$=0.318.

## CONCLUSIONS AND FUTURE WORK

A multiple-point statistics method using 2D thin sections to generate 3D pore-space representations of the carbonate rock has been tested in this paper. The microstructures of the carbonate rock were reconstructed and their permeabilities simulated by the lattice-Boltzmann method were compared with the experimental values. The predicted permeabilities were overestimated within a factor of three; however, the result is good considering the significant size difference between reconstructed images and the experimental sample. In this study, a combination of a small 2D image and a 9×9 template with multigrid simulation was successful to capture typical patterns seen in the 2D image. However, for more heterogeneous samples more information is needed. The reconstruction can be improved using additional information, such as higher-order information with large templates and several thin-section images including multi-orientation images if the medium is anisotropic, at the expense of more computer power and memory.

Future work will be devoted to application of the method to more carbonates, as well as the generation of topologically equivalent networks from 3D images. From the networks, predictions of capillary pressure and relative permeabilities for samples of arbitrary wettability can be made using pore-scale modeling [1].

## ACKNOWLEDGEMENTS

The authors would like to express their gratitude to Japan Oil, Gas and Metals National Corporation (JOGMEC) for financial and technical support of our research and to acknowledge JOGMEC for granting permission to publish this paper with the use of the lattice-Boltzmann simulation code. We thank David Stern (ExxonMobil) and Pål-Eric Øren (Statoil) for sharing the experimental data set with us and Peter Lock for providing the code for the effective medium approximation. We also thank the sponsors of the Imperial College Consortium on Pore-Scale Modelling for financial support.

## REFERENCES

1. Blunt, M.J., M.D. Jackson, M. Piri, and P.H. Valvatne, Detailed physics, predictive capabilities and macroscopic consequences for pore-network models of multiphase flow. *Advances in Water Resources*, (2002) **25**, 8-12, 1069-1089.
2. Chen, S. and G.D. Doolen, Lattice Boltzmann method for fluid flows. *Annual Review of Fluid Mechanics*, (1998) **30**, 329-364.
3. Dullien, F.A.L., *Porous Media: Fluid Transport and Pore Structure*, Academic Press, San Diego, (1992).
4. Ishida, H., Observation of Micro-Fabric of Source Rock by Focused Ion-Beam Workstation. *Annual Report of TRC's activities, Japan National Oil Corporation*, (1997) 115-119.
5. Tomutsa, L. and V. Radmilovic, Focussed Ion Beam Assisted Three-dimensional rock Imaging at Submicron-scale. *International Symposium of the Society of Core Analysts*, (2003) SCA2003-47.
6. Spanne, P., J.F. Thovert, C.J. Jacquin, W.B. Lindquist, K.W. Jones, and P.M. Adler, Synchrotron Computed Microtomography of Porous-Media - Topology and Transports. *Physical Review Letters*, (1994) **73**, 14, 2001-2004.
7. Fredrich, J.T., 3D imaging of porous media using laser scanning confocal microscopy with application to microscale transport processes. *Physics and Chemistry of the Earth Part A-Solid Earth and Geodesy*, (1999) **24**, 7, 551-561.

8. Bryant, S. and M. Blunt, Prediction of Relative Permeability in Simple Porous-Media. *Physical Review A*, (1992) **46**, 4, 2004-2011.
9. Bakke, S. and P.E. Øren, 3-D pore-scale modelling of sandstones and flow simulations in the pore networks. *SPE Journal*, (1997) **2**, 2, 136-149.
10. Pilotti, M., Reconstruction of clastic porous media. *Transport in Porous Media*, (2000) **41**, 3, 359-364.
11. Lucia, F.J., *Carbonate reservoir characterization*, Springer, Berlin, Germany, (1999).
12. Okabe, H. and M.J. Blunt, Multiple-Point Statistics to Generate Geologically Realistic Pore-Space Representations. *International Symposium of the Society of Core Analysts*, (2003) SCA2003-09.
13. Strebelle, S., K. Payrazyan, and J. Caers, Modeling of a deepwater turbidite reservoir conditional to seismic data using principal component analysis and multiple-point geostatistics. *SPE Journal*, (2003) **8**, 3, 227-235.
14. Caers, J., Geostatistical reservoir modelling using statistical pattern recognition. *Journal of Petroleum Science and Engineering*, (2001) **29**, 3-4, 177-188.
15. Lock, P.A., X.D. Jing, R.W. Zimmerman, and E.M. Schlueter, Predicting the permeability of sandstone from image analysis of pore structure. *Journal of Applied Physics*, (2002) **92**, 10, 6311-6319.
16. Koplik, J., Creeping Flow in Two-Dimensional Networks. *Journal of Fluid Mechanics*, (1982) **119**, JUN, 219-247.
17. Jurgawczynski, M., R.W. Zimmerman, and X.D. Jing, Estimating the permeability of carbonate rocks using image analysis and effective medium theory. *International Symposium of the Society of Core Analysts*, (2004).
18. Buckles, J.J., R.D. Hazlett, S.Y. Chen, K.G. Eggert, and W.E. Soll, Toward Improved Prediction of Reservoir Flow Performance - simulating oil and water flows at the pore scale. *Los Alamos Science*, (1994) **22**, 112-120.
19. Grunau, D., S.Y. Chen, and K. Eggert, A Lattice Boltzmann Model for Multiphase Fluid-Flows. *Physics of Fluids a-Fluid Dynamics*, (1993) **5**, 10, 2557-2562.
20. JNOC, Research on the quantitative analysis of multiphase flow dynamics in porous media using microscopic simulation approach. 2003.

21. Bhatnagar, P.L., E.P. Gross, and M. Krook, A model for collision processes in gases. I: small amplitude processes in charged and neutral one-component system. *Physical Review*, (1954) **94**, 3, 511-525.
22. Oshita, T. and H. Okabe, Early water breakthrough in carbonate core samples visualized with X-ray CT. *International Symposium of the Society of Core Analysts*, (2000) SCA2000-08.